Minimizing Power Loss of Hybrid Quadra Tied Solar PV Arrays Using Cuckoo Search MPPT Algorithm During Shading Scenarios

Abhinav BHATTACHARJEE and Suresh MIKKILI

***Abstract*—This study assists in selecting the appropriate solar photovoltaic (SPV) array configuration and metaheuristic maximum power point tracking (MPPT) technique to minimise power loss in rooftop SPV systems resulting from partial shading conditions (PSCs) caused by tall adjacent buildings in urban environments. A hybrid SPV array configuration, termed alternate – quadra tied – cross tied (A-QT-CT), that integrates quadra tied (QT) and total cross tied (TCT) configurations is proposed. This configuration is designed to provide maximum power extraction comparable to the best performing TCT configuration, while incorporating a reduced number of cross-links. Simulations were conducted utilising MATLAB to evaluate the performance of these configurations in the context of typical PSCs found in urban environments. This evaluation includes a comparative analysis with the established TCT, series-parallel (SP), bridge linked – TCT (BL-TCT), and SP-TCT configurations. The proposed configurations are integrated with Perturb & Observe (P&O), Cuckoo Search (CS), and Particle Swarm Optimisation (PSO) MPPT techniques. These algorithms were evaluated under PSCs using MATLAB simulations, as well as a hardware model implemented with the Texas Instruments TMS320F28379D microcontroller. The time required to track the MPP and the steady-state MPPT efficiency are assessed. The combination of the CS MPPT method with A-QT-CT and TCT configurations has been identified as the optimal solution for minimising power loss in this application.**

***Index Terms*—Alternate – quadra tied – cross tied, Cuckoo Search, hybrid PV array configuration, maximum power point tracking, partial shading, Particle Swarm Optimization, quadra tied, total cross tied.**

I. Introduction

THE primary variable influencing the power output of a solar photovoltaic (SPV) system is solar insolation (G), measured in Watts per square meter (W/m^2). This research work aims to address the issue of changing solar insolation and its impact on the power output from SPV systems. The occurrence of partial shading on the SPV array impacts insolation levels and significantly reduces the power output generated by the array. In many instances, partial shading can be mitigated by carefully selecting the installation site of the SPV array. However, in densely populated urban environments, it is becoming progressively challenging to eliminate the shading effect caused by adjacent tall buildings. This research work focusses on minimising power loss in rooftop SPV arrays, which is attributed to partial shading from adjacent tall buildings.

The initial strategy investigated by researchers to alleviate the negative impacts of partial shading conditions (PSCs) involves the configuration design of the SPV array. The primary parameter to consider when developing SPV array configurations is the necessity for achieving the highest global maximum power point (GMPP) across the range of potential PSCs that may be encountered. The secondary and tertiary considerations include the necessity for a minimal number of interconnections or cross-links to optimise conductor material usage and reduce wiring complexity, as well as maintaining a minimal number of local maximum power points (LMPP) in the power-voltage (P-V) curve when addressing PSCs. Table I presents an overview of recent advancements in the development of SPV array configurations. It has been observed that a majority of papers have not addressed specific applications in the selection of PSCs. In certain instances, generalisations have been made based on the degree of shading on the array, while the shading pattern has been overlooked. This represents a research gap that we aim to address in our application.

The second approach to mitigate the adverse effects of partial shading in recent times involves the reconfiguration of SPV arrays. A comprehensive review of recent reconfiguration techniques available in the literature is presented in [1] and [2]. Static reconfiguration techniques demonstrate superior power extraction capabilities compared to conventional SPV array configurations. However, the additional wiring requirements and associated complexity render them impractical for large arrays. Conversely, dynamic reconfiguration, which theoretically maximises power extraction, is often not favoured in practical applications due to the necessity for a significant number of switches, along with the resulting switching and conduction losses, as well as the costs linked to additional components.

The final component in optimising power extraction from SPV arrays involves the implementation of maximum

Manuscript received April 23, 2025; revised June 28, 2025 and August 8, 2025; accepted August 24, 2025. Date of publication December 30, 2025; date of current version September 9, 2025. *(Corresponding author: Suresh Mikkili.)*

Both authors are with the Electrical & Electronics Engineering Department, National Institute of Technology, Goa 403703, India (e-mail: abhinavbhattacharjee@yahoo.com; mikkili.suresh@nitgoa.ac.in).

Digital Object Identifier 10.24295/CPSSTPEA.2025.00032

TABLE I
LITERATURE REVIEW OF SPV ARRAY CONFIGURATIONS

No.	Research contribution/Outcome	Highlights/Observations/Research gaps
[3] [4]	The TCT configuration offers the highest maximum power extraction on average over a wide range of PSCs.	TCT is used as a benchmark for comparing the performance of all other SPV array configurations.
[5]	6×6 Benzene configuration is proposed that has 20 cross-links compared to 25 cross-links of an equivalent sized TCT SPV array while extracting maximum power in the same range as the latter.	Testing is done under very light shading conditions which are different from those encountered in urban areas in the real world.
[6]	7×7 Triple Tied array is proposed which has 33% less cross links compared to an equivalent size TCT array. Maximum power extracted is also always lesser than TCT.	Shading conditions chosen are not suitable for urban areas.
[7]	A 9×9 triple tied-cross linked (TT-CL) SPV array is tested which offers maximum power extraction second only to TCT.	The connection pattern of the array is not applicable for arrays smaller than 9×9.
[8]	Comprehensive performance analysis of 6x6 basic SPV array configurations - Series (S), Parallel (P), SP, BL, HC, TCT and hybrid configurations formed out of these namely SP-CT, BL-CT, HC-CT, SP-TCT, BL-TCT, HC-TCT, BL-HC.	SP-TCT, BL-TCT, HC-TCT, BL-HC hybrid configurations described here don't have a symmetrical design. Therefore, their performance will vary for the same kind of shade shape depending on location of the shade on the array.
[9]	9×9 conventional and hybrid configurations based on SP, BL, and TCT are examined under different PSCs caused by neighbouring buildings and clouds. It is shown that in cases where the percentage of partial shading is less than 30%, the SP configuration extracts maximum power from the array while in case of partial shading above 30%, the TCT configuration extracts maximum power from the array.	The research work doesn't consider the critical significance of shadow pattern in determining maximum power extraction from the array. Generalizing the perform ance of the configuration based on percentage of shading doesn't always work.
[10]	Mounting panels in a landscape orientation in the array can improve power extraction compared to portrait orientation as losses due to accumulation of dirt on the modules is reduced.	Can be applied to all the SPV array configurations.

TABLE II
LITERATURE REVIEW OF MPPT TECHNIQUES

No.	Research contribution/Outcome	Highlights/Observations/Research gaps
[11]	MPSO-MPC method is developed where INC method is aided by PSO in searching for the global peak. It is shown to perform better than PSO and CS algorithms.	Experimental analysis is done with only 2 series connected SPV modules. Performance with PSCs having multiple LMPPs is not known.
[12]	A modified P&O algorithm is proposed which scans the current -voltage (I -V) curve of the SPV array to determine likely location of the global peak to begin search for the GMPP. It has been implemented using a buck -boost converter and is shown to track MPP faster than PSO, Jaya and Ajaya MPPT techniques.	Analysis done with 4×2 SPV array. Its performance with large arrays is unknown as the algorithm requires high computational capabilities.
[13]	MPSO-HALS method is developed, where the PSO method is modified to initialize an evenly distributed population along the P-V curve. The population is further partitioned to choose the best half for global and local search. Adaptive step sizes are also introduced to improve search speed while reducing oscillations in the steady state thus combining the benefits of the P&O and PSO methods on which it is based.	The P-V curves used for experimentation are created using only 2 SPV modules, thus performance with large arrays having multiple LMPPs is not known.
[14]	A deep study of the PSO technique is done using pole-zero analysis for varying value of tuning constants. Further, a technique to find the convex area of the P-V curve is developed which aids the GMPP search.	Testing is done with P-V curves having up to 2 distinct peaks. The performance of the algorithm with large arrays having multiple LMPPs in close proximity is unknown as it requires high computational capabilities.
[15]	A hermite interpolation based strategy is proposed and shown to perform better than PSO and INC methods.	The algorithm is tested under PSCs with only 3 series connected SPV modules. The performance of the MPPT algorithm with large arrays having multiple LMPPs is therefore unknown as the algorithm requires high computational capabilities.
[16]	An ant colony optimization (ACO) and FL combined approach to MPPT called AFO is presented, and its performance is compared with ACO, FL and PSO.	The P-V curves are chosen randomly to mimic PSCs. The performance of the MPPT algorithm with large arrays having multiple LMPPs in close proximity is unknown.
[17]	Salp swarm algorithm (SSA) based MPPT is proposed and compared with hill climbing, butterfly optimization algorithm (BOA), grasshopper optimization algorithm (GOA), grey wolf optimization (GWO) and PSO.	Testing is done with 4×3 SPV array in simulation and 4×1 SPV array experimentally. The performance of the MPPT algorithm with large arrays having multiple LMPPs in close proximity is unknown.
[18]	An algorithm that tracks MPP using mathematical equations instead of search-based approach is developed.	The method's performance with large arrays where determining mathematical equations to represent the PV array voltage and current is complex is not known.
[19]	A real time deterministic peak hopping MPPT algorithm is developed and tested with complex PSCs having 5 or more peaks. Performance has been compared with intelligent-GWO, improved team game optimization (ITGA), SSA, modified deterministic Jaya (DM-JAYA) and MPSO-HALS algorithms.	The paper provides useful insight into the performance of multiple recent MPPT algorithms under complex PSCs having multiple peaks.
[20]	Rat swarm optimization (RSO) technique incorporated with PSC detection technique is designed to trigger RSO only when PSC is detected and MPP is detected under uniform shading conditions (USC) analytically.	The method used for detecting MPP under USC is susceptible to change in system parameters due to temperature variation and would need re-calibration. The PSC detection technique can be incorporated with any MPPT algorithm.

power point tracking (MPPT) algorithms, which ensure that the operating point of the SPV array aligns with the GMPP. Conventional strategies, including Perturb & Observe (P&O), incremental conductance (INC), and hill climbing, are straight forward to implement and enable rapid tracking of the MPP. However, these methods often become trapped at LMPPs.

In contrast, metaheuristic algorithms, which draw inspiration from various natural phenomena, are capable of tracking the GMPP under PSCs, although they exhibit slower convergence rates compared to the aforementioned techniques. A literature review of recent MPPT techniques proposed by researchers to address the PSC problem is provided in Table II. Some strategies involve hybrid methods where a combination of metaheuristic and conventional strategies are used to leverage the strengths of each individual strategy. It is observed that in most of the recent research work, testing has been done by using only a few PV modules which provide a limited scope to test the algorithms on multiple P-V curves with a high number of LMPPs as encountered in our chosen application. This is another gap which we have tried to address in our testing where the simulations and experimental tests have been both performed using a moderately large sized 8×8 SPV array.

The MPPT algorithms chosen for analysis are the P&O, CS and Particle Swarm Optimisation (PSO). The P&O algorithm is the simplest and most used MPPT method. The CS algorithm has been shown in literature to give good results for continuous optimization problems such as MPPT under PSCs [21], [22]. The PSO is one of the oldest metaheuristic algorithms and can be extensively modified to be adapted to a wide range of problems. The P&O and PSO serve as a benchmark to compare the performance of the CS algorithm. Hybrid algorithms mentioned in literature review have been avoided as it is intended to be able to run the algorithms reliably on a basic microcontroller without needing large processing capability.

Thus, the work done in this paper is presented in the following subsections: Section II features the modelling of PSCs encountered in urban areas. The modeling of the SPV array configurations is provided in Section III. Section IV illustrates the P-V and I-V curves obtained when the SPV array configurations encounter PSCs. Section V explains the working of the metaheuristic MPPT algorithms analyzed. Section VI has experimental tests performed to assess the MPPT algorithms. Section VII provides concluding remarks on the findings of the research.

II. PSCs Encountered and Their Modelling

On observing the shadow patterns caused due to buildings which are largely rectangular, it is evident that most of the shadows are rectangular, triangular or in between the two in the form of a trapezium. The shadows interchange between these shapes as the time of the day and day of the year change. We also notice many instances of random shaped shading which may be caused due to some fixtures being installed on the buildings, accumulation of dirt or debris on the modules, and clouds. Therefore, we have modeled the PSCs based on these cases as illustrated in Fig. 1. Three different random shading cases are chosen, with 'Random 1' representing light shading, 'Random 2' representing moderately heavy shading and 'Random 3' illustrating very heavy shading with one side being more heavily shaded than the other. The three random shading cases are also used to simulate progressive increase in shading on the array due to the motion of clouds using dynamic MPPT tests discussed in Section VI. An 8×8 sized SPV array is chosen for analysis considering the area available on the rooftop of a moderately sized apartment or office complex.

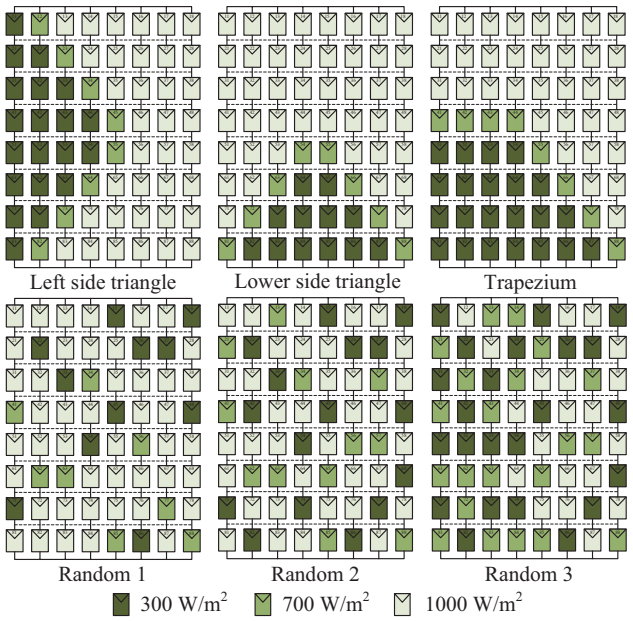

Fig. 1. Modelling of PSCs encountered in urban areas.

III. SPV Array Configurations Analyzed

This research work proposes a hybrid 8×8 SPV array configuration designated as alternate-quarda tied-cross tied (A-QT-CT). The configuration comprises alternating rows featuring Quadra tied connections, which are interspersed with rows that include a total cross link. The performance is evaluated in comparison to the quarda tied (QT) and total cross tied (TCT) configurations that serve as its foundation. The most commonly utilised series-parallel (SP) configuration has also been incorporated. SP configuration necessitates minimal conductor material due to the absence of cross-links, making it the simplest option for wiring and the most cost-effective. It experiences significant power loss under distributed shading conditions because there are insufficient parallel paths for current flow. The TCT configuration features cross-links between each module in the array, necessitating the highest amount of conductor material. The system delivers optimal performance across a diverse array of PSCs, demonstrating particular efficacy in scenarios involving random pattern PSCs. This effectiveness is attributed to the multiple current pathways it facilitates for current flow. Two other hybrid configurations, SP-TCT and bridge linked-TCT (BL-TCT) have also been analyzed to gauge the performance of the A-QT-CT configuration.

Fig. 2 depicts a general 8×8 SPV array configuration with

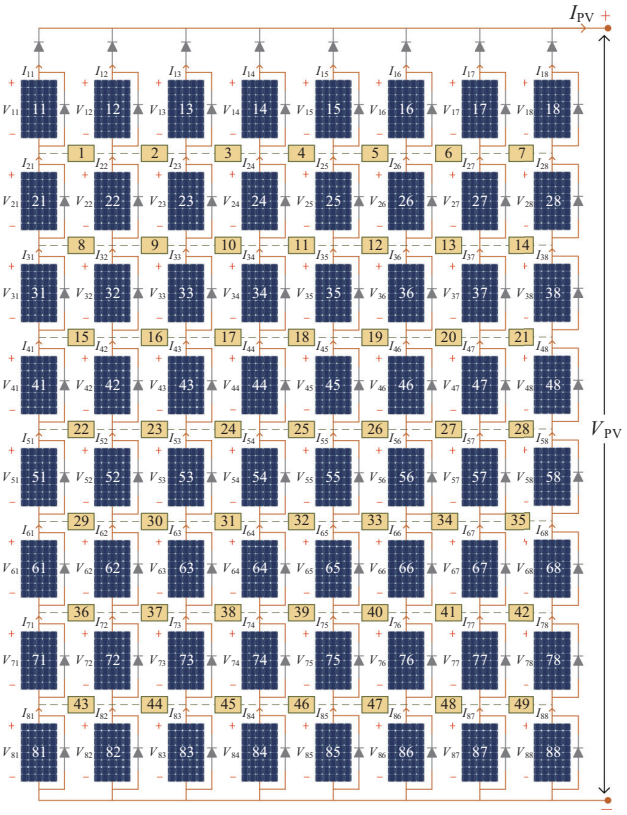

Fig. 2. Illustration of cross-link numbers in SPV arrays.

numbers allotted to every cross-link. The cross-link numbers which are present in each configuration along with the total number of cross-links are provided in Table III. The output voltage (V_{PV}) and current (I_{PV}) of the 8×8 SPV arrays are given in (1) where '*i*' and '*j*' stand for the row number and the column number of SPV array as per Fig. 2. The power output of the array (P_{PV}) is given by the product of V_{PV} and I_{PV}.

$$V_{PV} = \sum_{i=1}^{8} V_{i8}; \quad I_{PV} = \sum_{j=1}^{8} I_{1j} \tag{1}$$

IV. Testing of SPV Array Configurations Under PSCs

The theoretical approach to analysing the impact of PSCs on the P-V and I-V curves of a SPV array is notably complex for big arrays. The analysis of a 2×2 TCT layout under PSCs is presented in [23]. The number and positioning of LMPPs can be ascertained through the voltage and current equations derived. It has been noted that, even for a minimum-sized 2×2 array, the equations governing output voltage and current are large, resulting in increased complexity for a solution. Consequently, simulating the SPV arrays under PSCs represents a superior method that yields precise results. The PV module used in the array is Waaree Energies WSM-315 whose parameters are given as follows: max power (P_M) = 315 W, open circuit voltage (V_{OC}) = 43 V, short circuit current (I_{SC}) = 9.77 A, MPP voltage (V_M) = 35 V, MPP current (I_M) = 9 A. An 8×8 array made with this module produces 20.2 kW

TABLE III
Cross-Link Details of SPV Array Configurations

Configuration	Cross-link number present with reference to Fig. 2	Total number of cross-links
SP	–	0
TCT	1–49	49
SP-TCT	8–14, 22–28, 36–42	21
BL-TCT	2, 4, 6, 8–14, 16, 18, 20, 22–28, 30, 32, 34, 36–42, 44, 46, 48	33
QT	1–3, 5–7, 9–11, 13–14, 15, 17–19, 21, 22–23, 25–27, 29–31, 33–35, 37–39, 41–42, 43, 45–47, 49	37
A-QT-CT	1–3, 5–14, 16–18, 20–29, 31–33, 35–44, 46–48	42

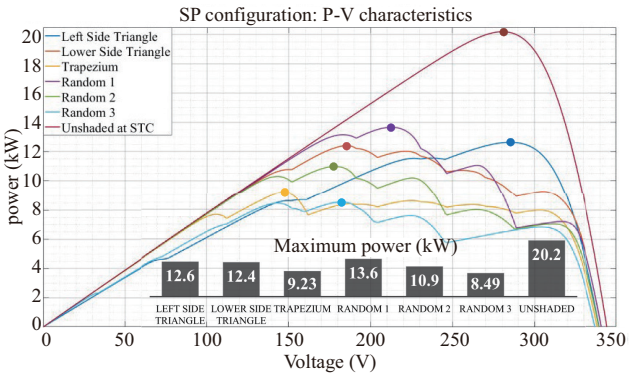

Fig. 3. P-V curves and P_M for SP array under PSCs.

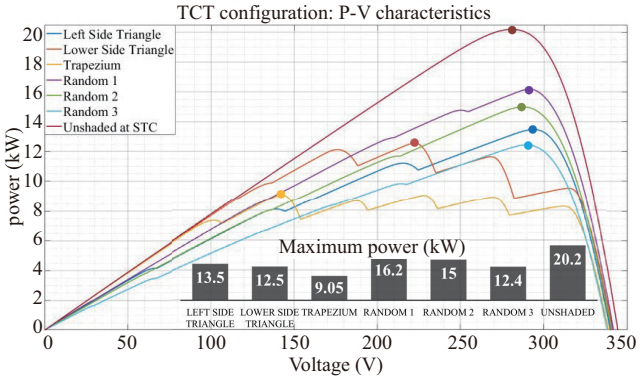

Fig. 4. P-V curves and P_M for TCT array under PSCs.

of maximum power under STC. The reason for choosing this module is that it is quite commonly used in rooftop installations and it is to be noted that the research results obtained in this paper are independent of the type of PV module being used. In this section, the P-V curves obtained by simulation using MATLAB for the SP, TCT, SP-TCT, BL-TCT, QT and A-QT-CT configurations under every PSC and unshaded condition are presented in Figs. 3–8 respectively. The maximum power extracted (P_M) under each case is also marked and mentioned in the above figures.

The analysis of P-V characteristics obtained under various PSCs confirms the enhanced performance of the TCT

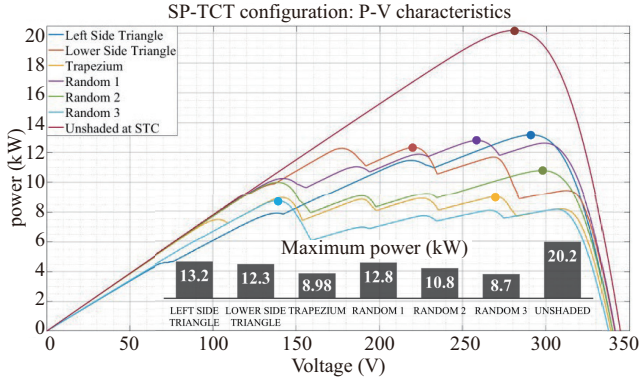

Fig. 5. P-V curves and P_M for SP-TCT array under PSCs.

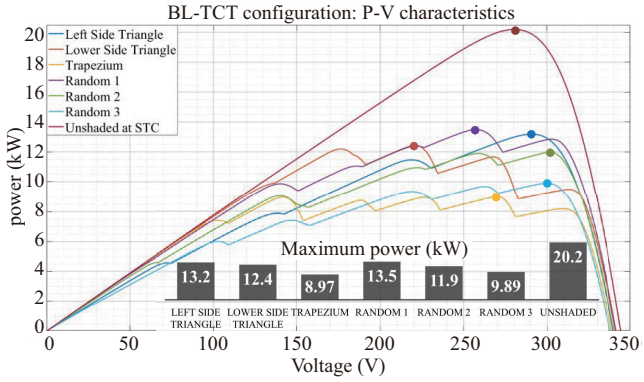

Fig. 6. P-V curves and P_M for BL-TCT array under PSCs.

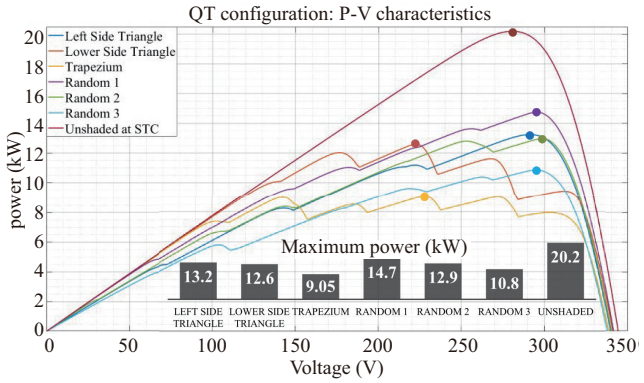

Fig. 7. P-V curves and P_M for QT array under PSCs.

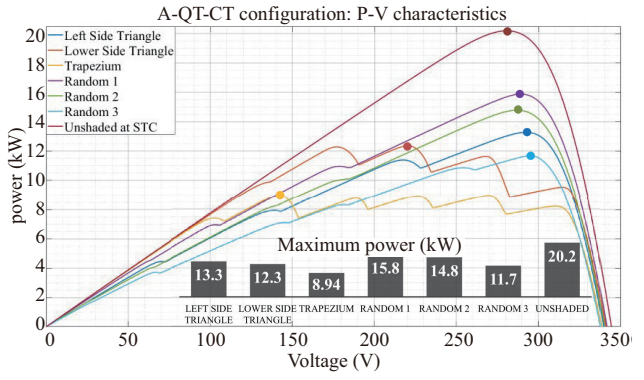

Fig. 8. P-V curves and P_M for A-QT-CT array under PSCs.

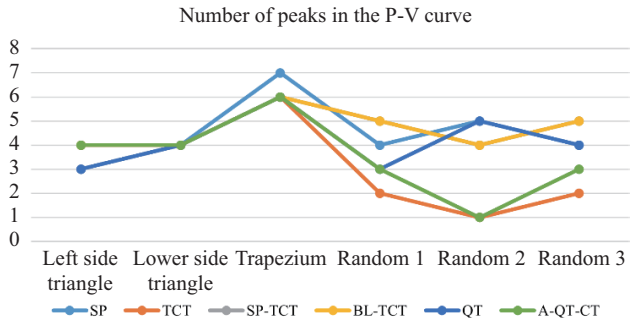

Fig. 9. Illustration of number of peaks in the P-V curves.

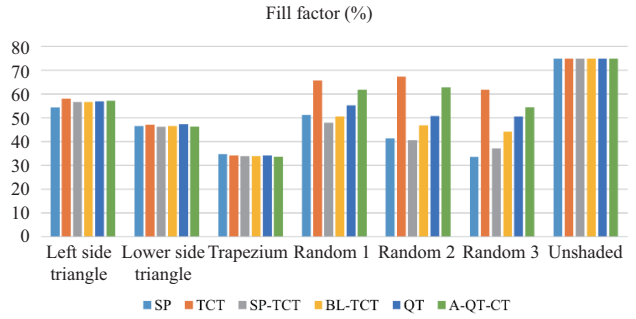

Fig. 10. Fill factor of the arrays under PSCs.

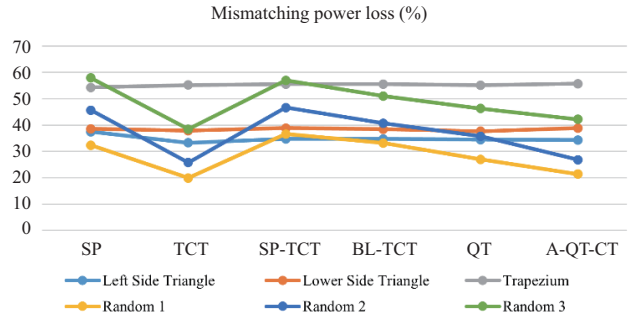

Fig. 11. Mismatching power loss of the arrays under PSCs.

configuration as it has an average P_M under PSCs of 13.12 kW while the A-QT-CT is second best with 12.82 kW. The remaining configurations in descending order of average P_M extraction are QT, BL-TCT, SP and SP-TCT with 12.25, 11.66, 11.23 and 11.13 kW, respectively. From Fig. 9 it can be observed that both TCT and A-QT-CT have the least number of peaks in the P-V curve under PSCs. These two configurations also have the highest fill factor and least mismatching power loss under PSCs as observed in Figs. 10 and 11. The A-QT-CT array also has 7 less cross-links than TCT for an 8×8 sized array which compensates for its slightly inferior performance compared to TCT. Therefore, these two configurations are chosen for analysis in Section VI to test the MPPT algorithms under the same PSCs and test the real-world power extraction capability of the combination.

V. Overview of the CS and PSO MPPT Techniques

We have considered two metaheuristics based MPPT algo-

rithms for comparison – CS and PSO, and P&O algorithm serves as a base to evaluate them.

The algorithms are also incorporated with an adjustable dwell time delay which can be used to adjust the speed of the duty cycle update process based on the limitations of system to get accurate tracking under all circumstances. This dwell time delay is not used in the software simulations but for the hardware tests, the duty cycle update process is made around 15 times slower than in the simulations by adjusting the dwell time to deal with the slow response of the system. The CS and PSO algorithms also check for change in irradiance in the array and restart the search for GMPP whenever PPV changes by 4% or above between successive measurements. This ensures the algorithms can track GMPP under dynamically changing PSCs, illustrated further in Section VI. The reason for choosing 4% as a threshold is that it provides an ideal balance between reacting to irradiance change and ensuring accurate tracking of GMPP without oscillation.

A. Cuckoo Search (CS) MPPT Technique

The CS optimisation method was developed based on the reproductive strategy of brood parasitism observed in cuckoo birds, which involves depositing their eggs in the nests of other host birds [24]. Cuckoos exhibit a strategic approach in selecting the timing for egg-laying, ensuring that their eggs hatch before those of the host bird. Upon hatching, cuckoos remove a portion of the host bird's eggs to increase the probability of their offspring obtaining sustenance. Host birds frequently identify and remove the eggs laid by cuckoos.

Identifying a suitable host bird's nest is critical for the reproductive strategy of the cuckoo. Fruit flies employ a sequence of linear flight trajectories, interspersed with abrupt 90° turns, to navigate their environment [25]. This flight pattern, referred to as Lévy flight is utilised by cuckoos for the purpose of identifying suitable nests for egg-laying. When used for MPPT, the mathematical representation of this process indicates that new solutions, denoted as 'd_{i+1}', are generated by cuckoos, as outlined in (2) [26].

$$d_{i+1}^{k} = d_{i}^{k} + \alpha \oplus Lévy(\lambda) \tag{2}$$

In this, 'd_i^k' represents the duty cycle sample, 'k' indicates the sample number, 'i' denotes the iteration number, 'α' signifies the positive step size selected by the designer, and '$\oplus$' indicates that 'α' is multiplied with each sample individually. A Lévy flight is mathematically characterised as a random walk where the step sizes are derived from the Lévy distribution, following a power law as described in (3), with 'l' representing the flight length and 'λ' denoting the variance, lying within the range $1 < \lambda < 3$. The process consists of numerous small steps and occasional significant leaps, attributable to the characteristics of the Lévy distribution. Extended jumps can significantly enhance the search efficiency of CS in particular contexts relative to other meta-heuristic algorithms.

$$Lévy(\lambda) \approx y = l^{-\lambda} \tag{3}$$

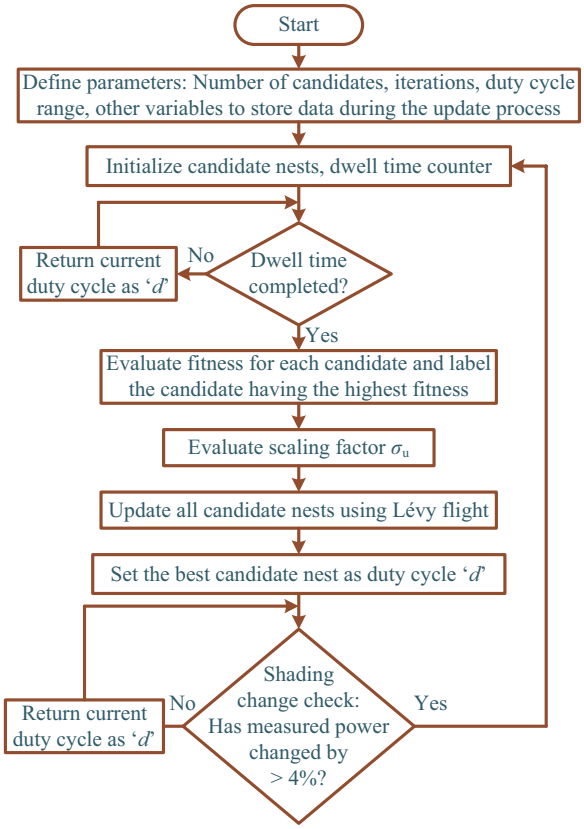

Fig. 12. Flow chart illustrating the CS MPPT algorithm.

The objective here is to optimise the fitness function, represented by the power output of the PV array calculated as the product of 'V_{pv}' and 'I_{pv}', through the selection of the optimal duty cycle 'd' for the DC-DC converter. (2) can be effectively applied as outlined in (4). The step size coefficient 'α' is set at 0.8, while 'β' is established at 1.5 after performing robustness analysis as discussed in Section VI.

$$d_{i+1}^{k} = d_{i}^{k} + \alpha \times \frac{|u|}{|v|^{1/\beta}} \times (d_{best} - d_{i}^{k}) \tag{4}$$

In the above equation, 'u' and 'v' are matrices having uniform distribution given by (5). 'σ_u' is defined by (6) and $\sigma_v = 1$. 'Γ' denotes the gamma operator.

$$\begin{cases} u \approx N(0, \sigma_u^2) \\ v \approx N(0, \sigma_v^2) \end{cases} \tag{5}$$

$$\sigma_u = \frac{\Gamma(1+\beta) \times \sin(\pi \times \frac{\beta}{2})}{\Gamma(\frac{1+\beta}{2}) \times \beta \times 2^{(\beta-1)/2}} \tag{6}$$

The execution of the CS algorithm for MPPT, as illustrated in Fig. 12, involves a procedure for selecting a nest that is comparable to identifying the optimal duty cycle for power maximisation. Four duty cycle values are initially selected from the search space. The fitness function value is utilised to eliminate the least effective duty cycles based on a specified

probability, determined by the condition that random number $r \in (0,1) > 0.25$ in this instance. This process is similar to the method of randomly destroying nests and eliminating eggs, while a new duty cycle is selected using the Lévy flight function. The procedure is performed in an iterative manner for a total of 20 iterations until the optimal duty cycle for maximising the SPV array power is determined.

B. PSO MPPT Technique

The PSO algorithm simulates the behaviour of a flock of birds in pursuit of an optimal food source [27], [28].

Each bird symbolises a solution, specifically the optimal duty cycle in this context. The location of an individual bird within a ock is influenced by the optimal bird in its immediate vicinity, referred to as 'P_{best}', as well as the most favourable solution identified by the entire flock, known as 'G_{best}'.When used for MPPT, the position of a bird is replaced by duty cycle and is updated by (7), where d_i^{t+1} is the updated duty cycle while d_i^t is the previous duty cycle. δ_i^{t+1} is the perturbation (δ) in current duty cycle. 'i' denotes the order number of the bird while 't' denotes the iteration number.

$$d_i^{t+1} = d_i^t + \delta_i^{t+1} \tag{7}$$

The updated perturbation in duty cycle is given by (8).

$$\delta_i^{t+1} = \omega\delta_i^t + c_1 r_1 (P_{best} - d_i^t) + c_2 r_2 (G_{best} - d_i^t) \tag{8}$$

where, 'ω' is inertia weight while 'c_1' and 'c_2' are the individual and social coefficients, taken as 1.0 and 1.2 respectively, after performing robustness analysis as discussed in Section VI. 'r_1' and 'r_2' are random numbers between 0 and 1. The inertia weight 'ω' is linearly decreased from 0.9 to 0.2 with every iteration 't' as given in (9). 'T' denotes the maximum iteration number.

$$\omega^t = \omega_{max} - \frac{t}{T}(\omega_{max} - \omega_{min}) \tag{9}$$

The flowchart of the PSO algorithm used to track MPP is illustrated in Fig. 13.

VI. Experimental Results

In this section, the two best performing SPV array configurations from Section IV – A-QT-CT and TCT are tested with P&O, CS and PSO MPPT methods under the six PSCs. Initially, simulations are performed using MATLAB where both SPV arrays are sequentially subjected to each PSC for 1 s before transitioning to the next. The parameters analyzed are MPPT efficiency, steady state oscillations and the time taken to achieve convergence. This is a better way to judge the performance of the MPPT algorithms' suitability for real world conditions than just measuring the time taken to converge under each PSC from a zero initial state as the results in the latter could vary if the values chosen for the initial variables are changed to suit every PSC. Fig. 14 provides the waveforms for the dynamic MPPT test for the A-QT-CT configuration.

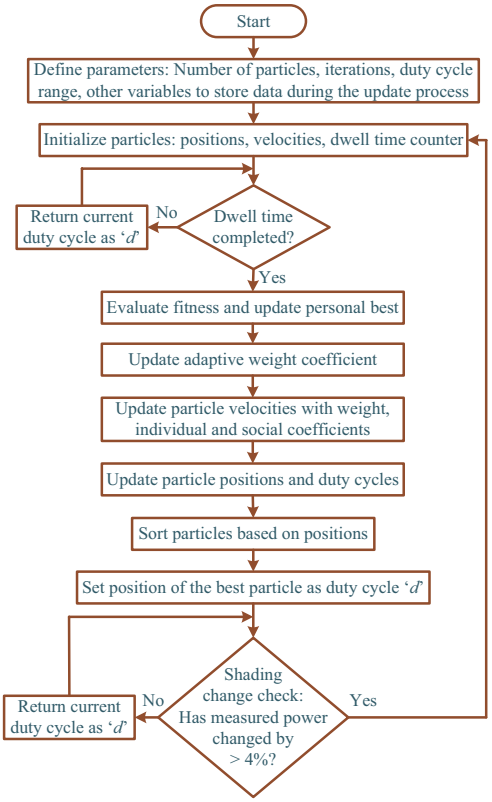

Fig. 13. Flowchart illustrating the PSO MPPT algorithm.

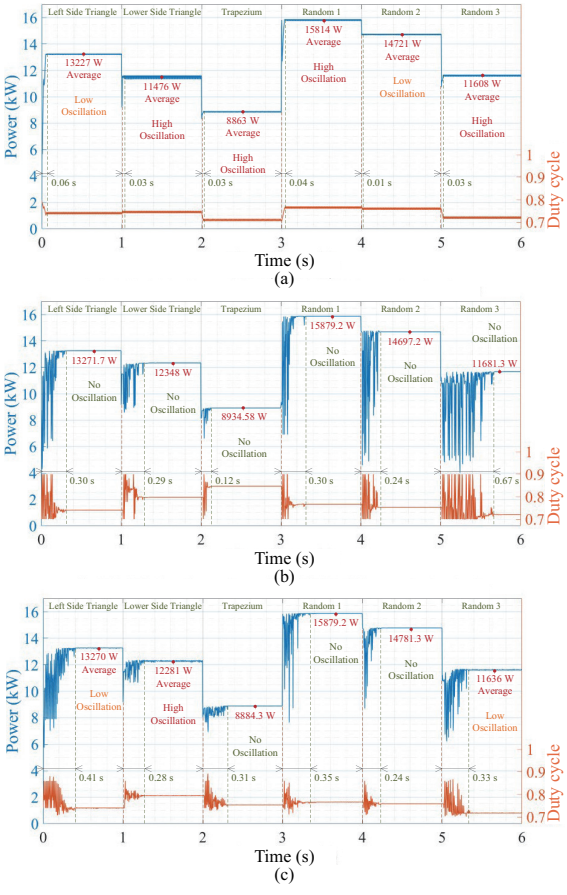

Fig. 14. Dynamic shading analysis of (a) P&O, (b) CS, and (c) PSO MPPT algorithms with A-QT-CT configuration.

TABLE IV
AVERAGE STEADY STATE MPPT EFFICIENCY (η) AND TIME TO TRACK MPP (T) – A-QT-CT CONFIGURATION (SIMULATION)

MPPT →	P&O		CS		PSO	
PSC ↓	η / %	T / s	η / %	T / s	η / %	T / s
Left side triangle	99.63	0.06	99.96	0.3	99.95	0.41
Lower side triangle	92.92	0.03	99.98	0.29	99.44	0.28
Trapezium	99.04	0.03	99.84	0.12	99.28	0.31
Random 1	99.55	0.04	99.96	0.3	99.96	0.35
Random 2	99.56	0.01	99.4	0.24	99.97	0.24
Random 3	99.34	0.03	99.97	0.67	99.58	0.33
Average	98.34	0.033	99.85	0.32	99.69	0.32

TABLE V
AVERAGE STEADY STATE MPPT EFFICIENCY AND TIME TO TRACK MPP – TCT CONFIGURATION (SIMULATION)

MPPT →	P&O		CS		PSO	
PSC ↓	η / %	T / s	η / %	T / s	η / %	T / s
Left side triangle	99.36	0.07	99.98	0.31	99.66	0.4
Lower side triangle	91.52	0.03	96.42	0.36	99.93	0.3
Trapezium	97.57	0.03	99.6	0.15	99.47	0.78
Random 1	99.18	0.06	99.98	0.29	99.79	0.4
Random 2	99.62	0.01	99.99	0.37	98.66	0.41
Random 3	99.62	0.02	99.95	0.16	99.93	0.85
Average	97.81	0.036	99.32	0.27	99.57	0.52

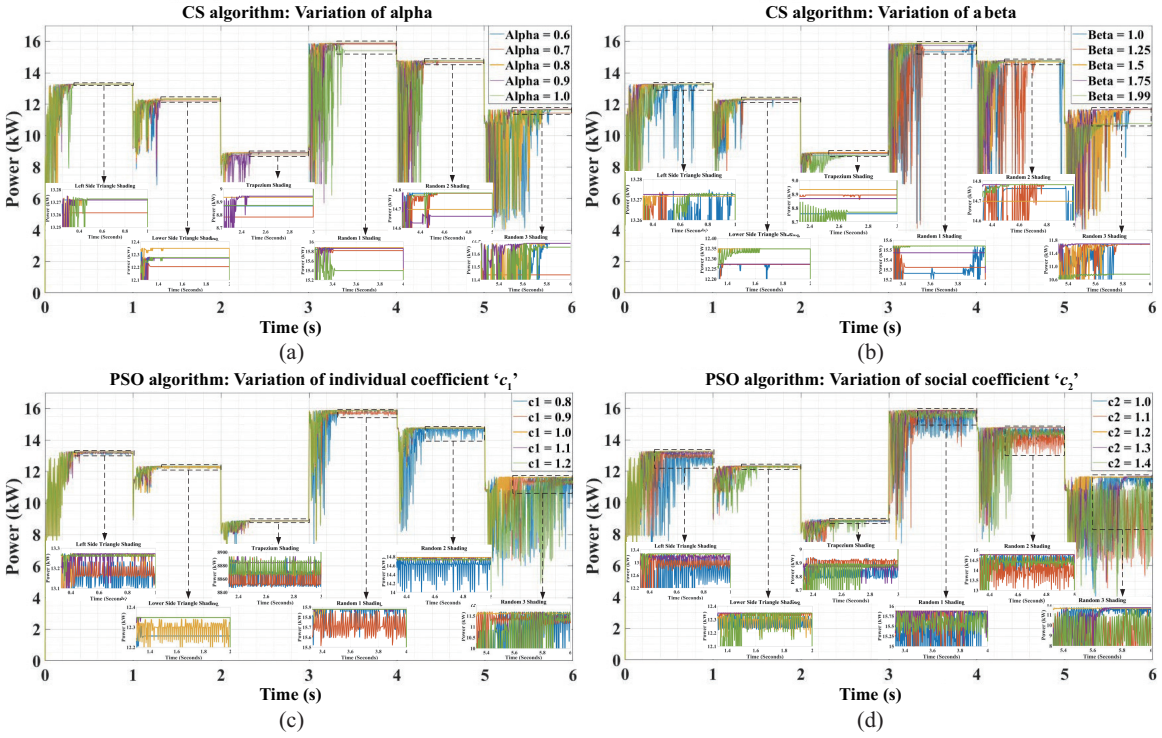

Fig. 15. Robustness analysis for the CS algorithm by varying (a) α, and (b) β, and the PSO algorithm by varying (c) c_1 and (d) c_2.

The maximum power tracked once convergence is achieved is labelled along with the quantum of oscillations present in the steady state. From this test, MPPT efficiency and time taken to converge for each new PSC case is determined and tabulated in Table IV. The same test is conducted for the TCT configuration and the results obtained are tabulated in Table V. It is observed that the CS algorithm performs the best in these tests as it shows no oscillation in the operating point once convergence is achieved while its tracking efficiency is the highest with the A-QT-CT configuration and slightly less than the PSO algorithm for the TCT configuration. The P&O algorithm is by far the fastest to converge, however it does get stuck at LMPP under one of the PSCs and shows continuous oscillation in the operating point even on convergence and as a result it has the least MPPT efficiency. The PSO method has a lower MPPT efficiency than the CS method for the A-QT-CT configuration while bettering the CS method's efficiency when tested with the TCT configuration. However, with the TCT configuration, the PSO algorithm shows heavy oscillation under Random 2 PSC. The PSO algorithm is also the slowest overall to converge to MPP.

Fig. 15 illustrates the robustness analysis of the tuning parameters chosen for the CS and PSO algorithms for the given system. Robustness analysis is performed by repeating the dynamic MPPT test with the A-QT-CT configuration while varying the tuning parameters of the CS algorithm - α and β, and PSO algorithm - c_1 and c_2. The results for the most optimum choice of parameters in all the cases are given in yellow and it is observed that these parameters offer a combination of high MPP, faster tracking and minimum steady state oscillations. For the CS algorithm, the optimum value of α is 0.8 and test results are provided in Fig. 15(a) for values

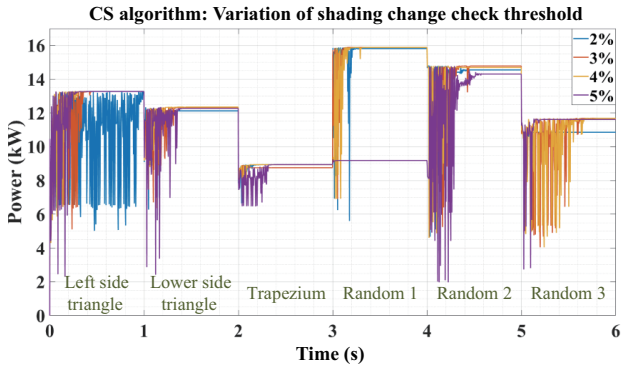

Fig. 16. Effect of varying the shading change check threshold.

of α ranging from 0.6 to 1 while keeping β constant at 1.5. Similarly, in Fig. 15(b), the test is repeated keeping α constant at 0.8 while β values are changed from 1.0 to 1.99. β = 1.5 gives the best results here and it is observed that performance significantly degrades for values of α and β outside these ranges. At β = 2.0, the algorithm fails to converge, hence the selection of β = 1.99 as the upper limit. Similarly, in Fig. 15(c) and (d), the dynamic MPPT test is carried out for different values of c_1 and c_2 respectively in the PSO algorithm. The parameters chosen here are kept the same while testing with the TCT configuration as well. This provides further validation of the robustness of the chosen parameters under different conditions. It is also noted that the performance of the PSO algorithm is more sensitive to parameter changes compared to the CS algorithm.

Another important factor is the setting of the shading change check threshold in CS and PSO algorithms. The effect of changing this threshold to restart the MPPT search which using the dynamic MPPT test for the CS algorithm is illustrated in Fig. 16, when significant shading change leading to change in PV array power is detected. Similar results are obtained with the PSO algorithm as well. It is observed that setting a low threshold of 2% leads to increased oscillation and non-convergence or slower convergence under some PSCs, as even minor oscillations in the PV power lead to restarting of the search process, while setting a high threshold of 5% leads to the algorithm not restarting the search process even under significant change in irradiation, as seen in the transition from trapezium to random 1 PSC. Therefore, in our application, a threshold value of 4% is chosen as it offers the best results while 3% can also be considered as the results are close.

The MPPT test is then performed using an experimental hardware model to evaluate real-world performance. The P-V curves generated by the SPV array configurations under PSCs are replicated utilising the Chroma Solar PV simulator model 62050H-600S. The MPPT algorithm is executed on the Texas Instruments TMS320F28379D microcontroller. Fig. 17 illustrates the experimental setup.

Two factors are evaluated to assess the performance of the MPPT algorithms. The initial metric is the MPPT efficiency over a duration of one minute, which serves as an indicator of the proximity of the operating point to the GMPP during

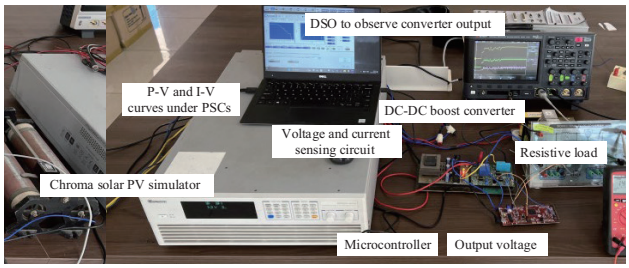

Fig. 17. Experimental setup for MPPT test.

steady-state operation. The steady state oscillation around the MPP is also taken into account in this metric. The second point of consideration is the duration required for the algorithm to reach the MPP. To ensure the MPPT test closely resembles real-world conditions, the dimensions of the SPV array and PSCs are maintained consistent with those utilised in the simulations conducted in Section IV. The power is reduced by a factor of 75 as a result of the hardware components' power limitations. The tests maintain the shape and number of peaks in the P-V curve while solely reducing the power level, thereby offering an accurate representation of the MPPT algorithm's performance in real-world conditions. These tests are performed five times for each configuration under each PSC to account for the randomness in the metaheuristic algorithms and the resulting change in results on every run. The average steady state MPPT efficiency and time taken to track MPP over 5 runs for the A-QT-CT configuration and TCT configuration are presented in Tables VI and VII respectively. It is observed that the MPPT efficiency of P&O algorithm is significantly lower in the hardware tests than in the dynamic MPPT tests in simulations. This is because the hardware tests have been conducted for each PSC separately. Therefore, the operating point often gets stuck at the first LMPP that it encounters as it starts scanning the P-V curve. In the simulations, the PSCs are sequentially applied one after the other and therefore the GMPP is tracked more often. In certain transitions, for example, from left side triangle to lower side triangle, where there is a greater difference in the duty cycle at which the MPP occurs for the PSCs, the P&O gets stuck at a LMPP after the PSC transition.

The MPPT test results for the A-QT-CT configuration under PSCs with P&O, CS and PSO MPPT algorithms for one of the runs are provided in Figs. 18–20 respectively. The MPPT efficiency during a 1 min test run is displayed on the Chroma SPV simulator interface, including the theoretical maximum power 'P_{mp}', V_{OC}, I_{SC}, maximum voltage (V_{mp}), maximum current (I_{mp}), and the measured average maximum power '$P_{average}$'. Additional parameters such as instantaneous voltage (V_{mea}), current (I_{mea}), and power (P_{mea}) are also visible. The time required for the algorithm to track the MPP is quantifiable by analysing the output voltage, current, and power waveforms of the DC-DC converter, as displayed on a digital storage oscilloscope (DSO).

The results obtained show the CS algorithm offers the best MPPT efficiency – around 0.6% higher than PSO while also being 0.8 s faster on an average to track MPP than the latter.

(a) Left side triangle shading

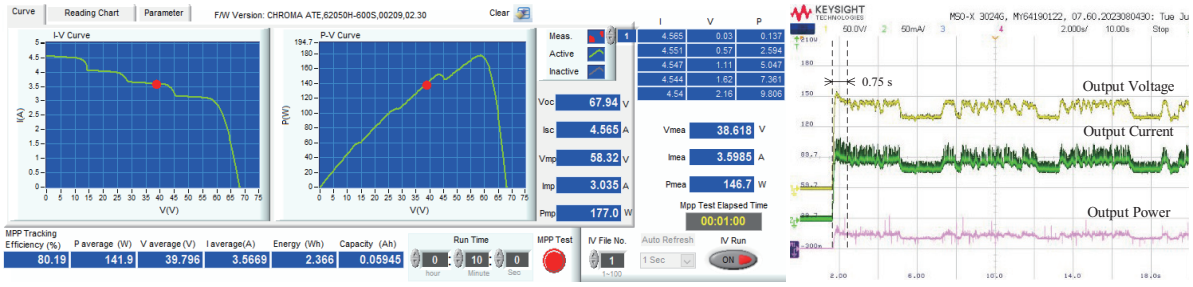

(b) Lower side triangle shading

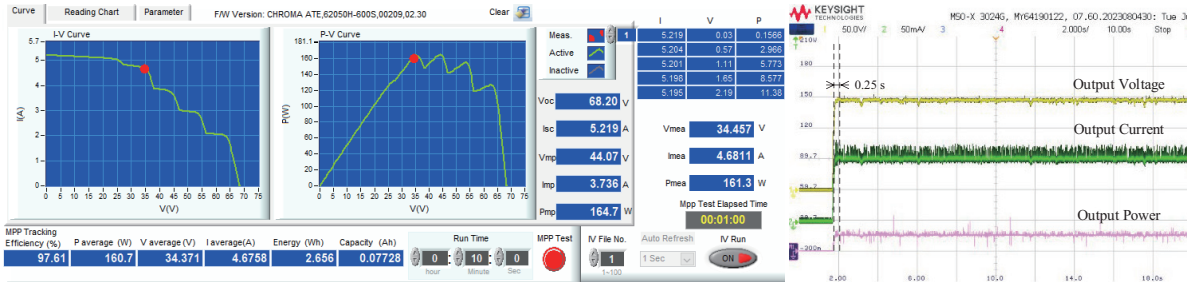

(c) Trapezium shading

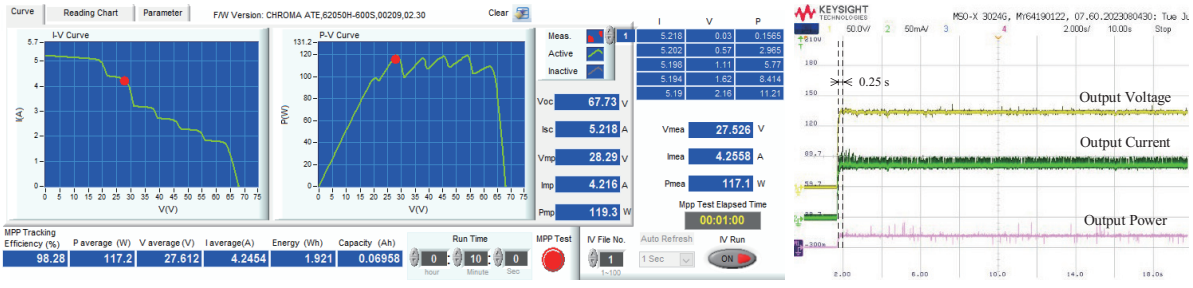

(d) Random 1 shading

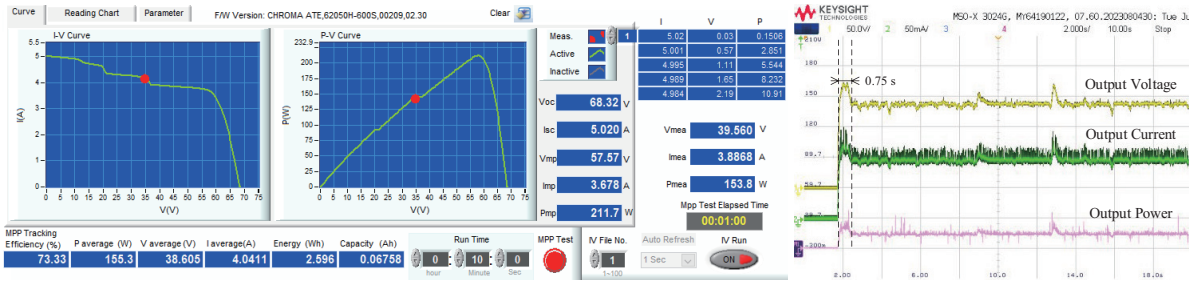

(e) Random 2 shading

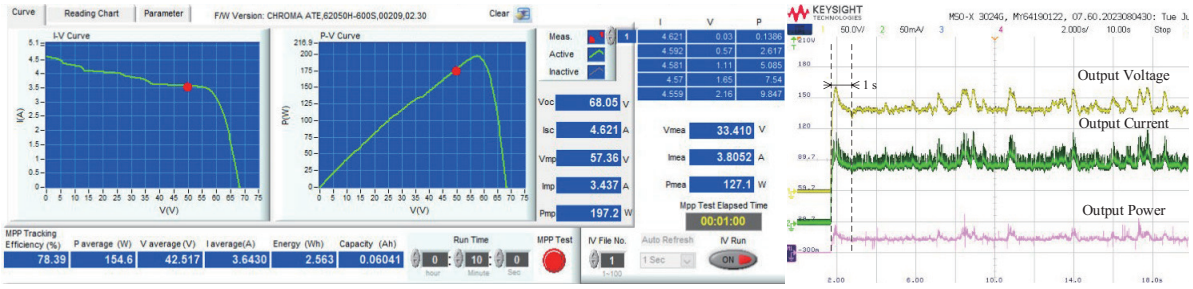

(f) Random 3 shading

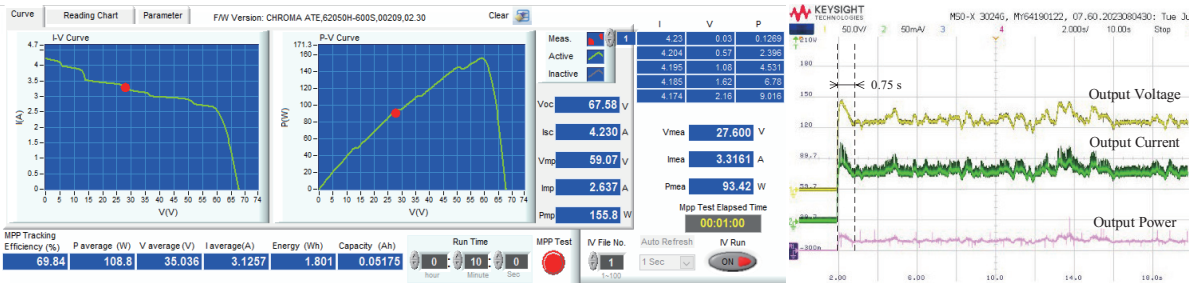

Fig. 18. Experimental hardware test results for A-QT-CT configuration with P&O MPPT algorithm.

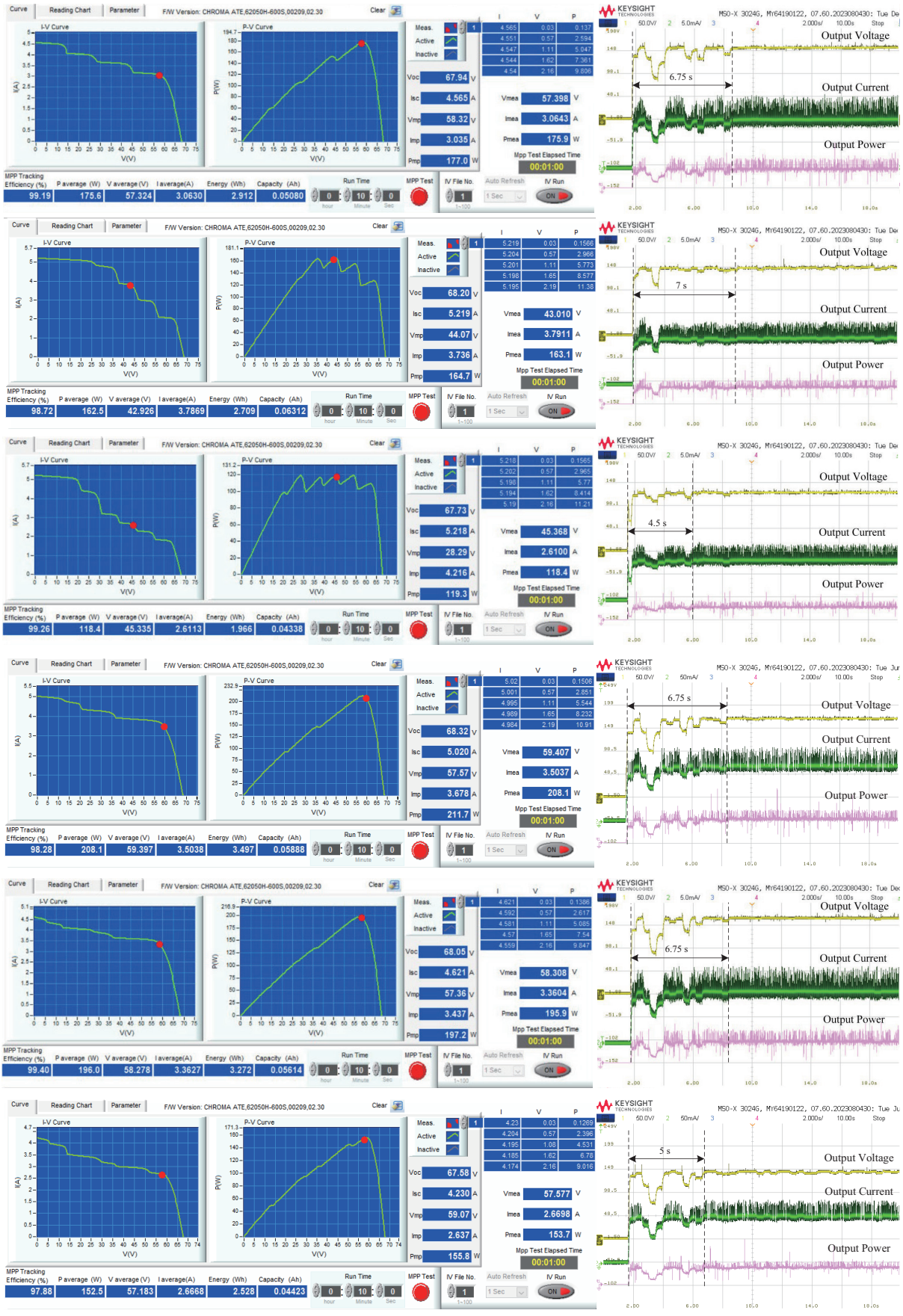

Fig. 19. Experimental hardware test results for A-QT-CT configuration with CS MPPT algorithm.

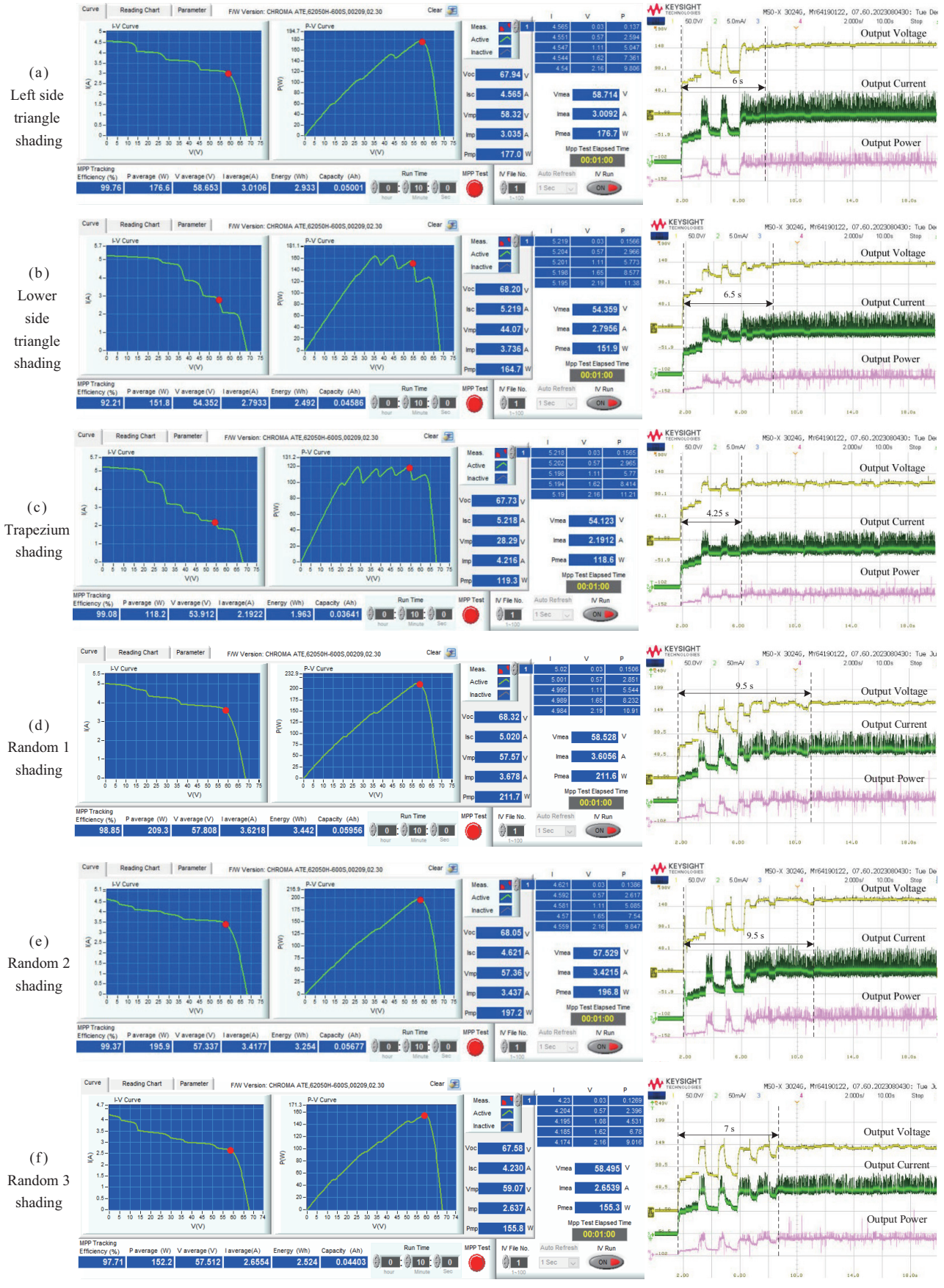

Fig. 20. Experimental hardware test results for A-QT-CT configuration with PSO MPPT algorithm.

TABLE VI
AVERAGE STEADY STATE MPPT EFFICIENCY AND TIME TO TRACK MPP – A-QT-CT CONFIGURATION (HARDWARE)

MPPT →	P&O		CS		PSO	
PSC ↓	η/%	T/s	η/%	T/s	η/%	T/s
Left side triangle	80.19	0.75	99.13	6.83	99.58	6.03
Lower side triangle	97.61	0.33	98.46	6.93	95.73	6.5
Trapezium	98.28	0.25	98.92	4.52	97.88	4.22
Random 1	73.33	0.75	98.45	6.63	99.01	9.5
Random 2	78.39	1	98.93	6.72	99.04	9.5
Random 3	69.84	0.75	97.52	5.04	98.31	6.75
Average	82.94	0.64	98.56	6.11	98.25	7.08

TABLE VII
AVERAGE STEADY STATE MPPT EFFICIENCY AND TIME TO TRACK MPP – TCT CONFIGURATION (HARDWARE)

MPPT →	P&O		CS		PSO	
PSC ↓	η/%	T/s	η/%	T/s	η/%	T/s
Left side triangle	75.38	0.75	99.5	6.78	99.1	7.25
Lower side triangle	94.84	0.33	99.3	7.25	94.07	6.78
Trapezium	98.35	0.5	98.62	6.67	96.89	4.33
Random 1	80.8	0.67	97.73	6.75	99.39	9.67
Random 2	78.54	1	98.81	6.5	99.18	9.5
Random 3	72.84	0.75	99.08	7.33	98.92	7.5
Average	83.45	0.67	98.84	6.88	97.92	7.51

The P&O method offers by far the quickest convergence, which is nearly 10 times faster than the metaheuristic MPPT techniques but fails to track MPP under 4 out of the 6 PSCs. This coupled with the continuous oscillation in the operating point even after convergence leads to a poor MPPT efficiency of around 83% compared to roughly above 98% that is offered by the CS and PSO algorithms. Between the CS and PSO algorithms, PSO has more oscillation and a tendency to get stuck at LMPP in cases where the GMPP is closely surrounded by multiple LMPP, such as lower side triangle shading. The results also prove that under very fast changing PSCs, where the PSC has changed even before the algorithm has converged for the previous PSC, the P&O method would track MPP more effectively than any of the metaheuristics-based algorithms. This remains a key disadvantage of all metaheuristic algorithms.

VII. CONCLUSION

The first focus area of the research is in the choice of suitable SPV array configuration for reduction of power loss due to PSCs in urban areas. In this, the A-QT-CT configuration offers a maximum power extraction of around 2% lesser on average than the best performing TCT configuration while having 15% lesser cross-links. The TCT configuration thus remains the best choice for rooftop applications, but A-QT-CT configuration comes very close and can be a valid contender. The choice of configuration between these two thus comes down to cost analysis of conductor material depending on size of the array and PSCs likely to be encountered. Amongst the MPPT strategies, the P&O method is by far the fastest, converging within 34 ms in the dynamic shading change simulation tests compared to the 295 ms and 420 ms taken by CS and PSO respectively. This is at the expense of MPPT efficiency as the P&O offers 98% unlike the CS and PSO which both offer 99.6%. In hardware experiments, the configurations, when used with the CS MPPT technique, offer superior performance than with the P&O and PSO MPPT techniques, as the CS method can track the GMPP most accurately. The CS algorithm offers 15.5% and 0.7% greater MPPT efficiency than the P&O and PSO algorithms respectively here while also being 0.8 faster than the PSO to converge. The P&O method is again much faster to converge here taking just under a second. The P&O and PSO algorithms suffer from oscillations in the operating point during steady state which is not the case with CS. The combination of CS MPPT method with TCT or A-QT-CT SPV array configuration are thus very suitable for application in rooftop SPV systems for the type of PSCs encountered in urban areas.

REFERENCES

[1] V. C. Chavan and S. Mikkili, "A typical review on static reconfiguration strategies in photovoltaic array under non-uniform shading conditions," in *CSEE Journal of Power and Energy Systems*, Jan. 2020.

[2] M. Jalal, I. U. Khalil, A. U. Haq, A. Flah, and S. a. M. A. Wahab, "Advancements in PV array reconfiguration techniques: Review article," in *IEEE Access*, p. 1, Jan. 2024.

[3] M. N. R. Nazer, A. Noorwali, M. F. N. Tajuddin, M. Z. Khan, M. A. I. A. Tazally, J. Ahmed, T. S. Babu, N. H. Ghazali, C. Chakraborty, and N. M. Kumar, "Scenario-based investigation on the effect of partial shading condition patterns for different static solar photovoltaic array configurations," in *IEEE Access*, vol. 9, pp. 116050–116072, Jan. 2021.

[4] R. K. Pachauri, O. P. Mahela, A. Sharma, J. Bai, Y. K. Chauhan, B. Khan, and H. H. Alhelou "Impact of partial shading on various PV array configurations and different modeling approaches: A comprehensive review," in *IEEE Access*, vol. 8, pp. 181375–181403, Jan. 2020.

[5] C. Saiprakash, A. Mohapatra, B. Nayak, T. S. Babu, and H. H. Alhelou, "A novel benzene structured array configuration for harnessing maximum power from PV array under partial shading condition with reduced number of cross ties," in *IEEE Access*, vol. 10, pp. 129712–129726, Jan. 2022.

[6] P. K. Bonthagorla and S. Mikkili, "A novel fixed PV array configuration for harvesting maximum power from shaded modules by reducing the number of cross-ties," in *IEEE Journal of Emerging and Selected Topics in Power Electronics*, vol. 9, no. 2, pp. 2109–2121, Mar. 2020.

[7] T. Ramesh, K. Rajani, and A. K. Panda, "A novel triple-tied-cross-linked PV array configuration with reduced number of cross-ties to extract maximum power under partial shading conditions," in *CSEE Journal of Power and Energy Systems*, Jan. 2020.

[8] S. R. Pendem, S. Mikkili, S. S. Rangarajan, S. Avv, R. E. Collins, and T. Senjyu, "Optimal hybrid PV array topologies to maximize the power output by reducing the effect of non-uniform operating conditions," in *Electronics*, vol. 10, no. 23, p. 3014, Dec. 2021.

[9] P. R. Satpathy, T. S. Babu, S. K. Shanmugam, L. N. Popavath, and H. H. Alhelou, "Impact of uneven shading by neighboring buildings and clouds on the conventional and hybrid configurations of roof-top PV arrays," in *IEEE Access*, vol. 9, pp. 139059–139073, Jan. 2021.

[10] H. Oufettoul, N. Lamdihine, S. Motahhir, N. Lamrini, I. A. Abdelmoula, and G. Aniba, "Comparative performance analysis of PV module positions in a solar PV array under partial shading conditions," in *IEEE Access*, vol. 11, pp. 12176–12194, Jan. 2023.

[11] M. A. Hendy, Mohamed. A. Nayel, J. Rodriguez, and M. Abdelrahem, "Enhanced maximum power point tracking using modified PSO hybrid

with MPC under partial shading conditions," in *IEEE Access*, p. 1, Jan. 2024.
[12] T. V. Anh, T. N. Trieu, P. V. H. Nghi, and B. Van Hien, "Fast and accurate GMPPT based on modified P&O algorithm," in *IEEE Access*, vol. 12, pp. 129588–129600, Jan. 2024.
[13] J. S. Koh, R. H. G. Tan, W. H. Lim, and N. M. L. Tan, "A modified particle swarm optimization for efficient maximum power point tracking under partial shading condition," in *IEEE Transactions on Sustainable Energy*, vol. 14, no. 3, pp. 1822–1834, Mar. 2023.
[14] R. Sangrody, S. Taheri, A. -M. Cretu, and E. Pouresmaeil, "An improved PSO-based MPPT technique using stability and steady state analyses under partial shading conditions," in *IEEE Transactions on Sustainable Energy*, vol. 15, no. 1, pp. 136–145, Jan. 2024.
[15] C. Yuan, J. Xia, F. Huang, P. Zhao, and L. Kong, "A novel hermite interpolation-based MPPT technique for photovoltaic systems under partial shading conditions," in *IEEE Photonics Journal*, vol. 16, no. 2, pp. 1–10, Feb. 2024.
[16] K. Xia, Y. Li, and B. Zhu, "Improved photovoltaic MPPT algorithm based on ant colony optimization and fuzzy logic under conditions of partial shading," in *IEEE Access*, vol. 12, pp. 44817–44825, Jan. 2024.
[17] M. N. I. Jamaludin, M. F. N. Tajuddin, J. Ahmed, A. Azmi, S. A. Azmi, and N. H. Ghazali, "An effective SALP swarm based MPPT for photovoltaic systems under dynamic and partial shading conditions," in *IEEE Access*, vol. 9, pp. 34570–34589, Jan. 2021.
[18] M. Etezadinejad, B. Asaei, S. Farhangi, and A. Anvari-Moghaddam, "An improved and fast MPPT algorithm for PV systems under partially shaded conditions," in *IEEE Transactions on Sustainable Energy*, vol. 13, no. 2, pp. 732–742, Nov. 2021.
[19] J. S. Koh, R. H. G. Tan, W. H. Lim, and N. M. L. Tan, "A real-time deterministic peak hopping maximum power point tracking algorithm for complex partial shading condition," in *IEEE Access*, vol. 12, pp. 43632–43644, Jan. 2024.
[20] K. K. Mohammed, S. Buyamin, I. Shams, and S. Mekhilef, "Hybrid global maximum power tracking method with partial shading detection technique for PV systems," in *IEEE Journal of Emerging and Selected Topics in Power Electronics*, vol. 10, no. 4, pp. 4821–4831, Nov. 2021.
[21] A. Ibrahim, R. Aboelsaud, and S. Obukhov, "Maximum power point tracking of partially shading PV system using cuckoo search algorithm," in *Proceedings of International Journal of Power Electronics and Drive Systems (IJPEDS)*, vol. 10, no. 2, p. 1081, Apr. 2019.
[22] M. I. Mosaad, M. O. A. El-Raouf, M. A. Al-Ahmar, and F. A. Banakher, "Maximum power point tracking of PV system based Cuckoo search algorithm; review and comparison," in *Energy Procedia*, vol. 162, pp. 117–126, Apr. 2019.
[23] S. Mohammadnejad, A. Khalafi, and S. M. Ahmadi, "Mathematical analysis of total-cross-tied photovoltaic array under partial shading condition and its comparison with other configurations," in *Solar Energy*, vol. 133, pp. 501–511, May 2016.
[24] Yang X.-S. and Deb S., "Cuckoo search via Lévy flights," in *Proceedings of Nature & Biologically Inspired Computing*, 2009, p. 210–214.
[25] A. M. Reynolds and M. A. Frye, "Free-flight odor tracking in drosophila is consistent with an optimal intermittent scale-free search," in *PloS One,* vol. 2, no. 4, p. e354, Apr. 2007.
[26] A. M. Eltamaly, "An improved Cuckoo search algorithm for maximum power point tracking of photovoltaic systems under partial shading conditions," in *Energies*, vol. 14, no. 4, p. 953, Feb. 2021.
[27] J. Kennedy and R. Eberhart, "Particle swarm optimization," in *Proceedings of ICNN'95 - International Conference on Neural Networks*, Perth, WA, Australia, 1995, pp. 1942–1948, vol. 4.
[28] Y. Shi and R. Eberhart, "A modified particle swarm optimizer," in *Proceedings of 1998 IEEE International Conference on Evolutionary Computation Proceedings. IEEE World Congress on Computational Intelligence*, Anchorage, AK, USA, 1998, pp. 69–73.

Abhinav Bhattacharjee received the B.E. degree in Electrical & Electronics Engineering from Goa College of Engineering, Farmagudi, Goa, India in 2014, and the M.Tech degree in power electronics and drives from Vellore Institute of Technology, Vellore, India in 2017. He joined as a Lecturer in Electrical Engineering at Government Polytechnic Bicholim, Goa, India, in 2017, and is currently pursuing his Ph.D. degree in electrical and electronics engineering at National Institute of Technology Goa, Cuncolim, India. His research interests include solar photovoltaic systems, DC-DC converters and applications of metaheuristic algorithms and soft computing techniques.

Suresh Mikkili obtained his M.Tech and Ph.D. degrees in Electrical Engineering from the National Institute of Technology, Rourkela in the years 2008 and 2013, respectively. He holds the position of Associate Professor in the Department of Electrical and Electronics Engineering (EEE) at the National Institute of Technology Goa (NIT Goa), India, starting from January 2013.

His research interests include smart electric grid, electric vehicles, grid connected/stand-alone PV systems, wireless power transfer, power quality issues and applications of soft computing techniques. He authored two books published by CRC Press, Taylor & Francis Group, in August 2015 and 2021, respectively. He has also authored the AICTE approved textbook titled "Power Systems-I" for B.Tech III year students. He has published over 135 papers in prestigious international journals (SCI/SCI-E) and international conferences. The government of India awarded him an Early Career Researcher Award.